Impact of symmetry on the ferroelectric properties of CaTiO3 thin films

Michael D. Biegalski, Liang Qiao, Yijia Gu, Apurva Mehta, Qian He, Yayoi Takamura, Albina Borisevich, and Long-Qing Chen

---

Articles you may be interested in

Impact of symmetry on the ferroelectric properties of CaTiO$_3$ thin films

Michael D. Biegalski,[1] Liang Qiao,[1,a)] Yijia Gu,[2] Apurva Mehta,[3] Qian He,[4]
Yayoi Takamura,[5,b)] Albina Borisevich,[4] and Long-Qing Chen[2]

[1]*Center for Nanophase Materials Sciences, Oak Ridge National Laboratory, Oak Ridge,
Tennessee 37831, USA*
[2]*Department of Materials Science and Engineering, Pennsylvania State University, University Park,
Pennsylvania 16801, USA*
[3]*Stanford Synchrotron Lightsource SLAC National Accelerator Laboratory, Menlo Park,
California 94025, USA*
[4]*Materials Science and Technology Division, Oak Ridge National Laboratory, Oak Ridge,
Tennessee 37831, USA*
[5]*Department of Chemical Engineering and Materials Science, University of California Davis, Davis,
California 95616, USA*

Epitaxial strain is a powerful tool to induce functional properties such as ferroelectricity in thin films of materials that do not possess ferroelectricity in bulk form. In this work, a ferroelectric state was stabilized in thin films of the incipient ferroelectric, CaTiO$_3$, through the careful control of the biaxial strain state and TiO$_6$ octahedral rotations. Detailed structural characterization was carried out by synchrotron x-ray diffraction and scanning transmission electron microscopy. CaTiO$_3$ films grown on La$_{0.18}$Sr$_{0.82}$Al$_{0.59}$Ta$_{0.41}$O$_3$ (LSAT) and NdGaO$_3$ (NGO) substrates experienced a 1.1% biaxial strain state but differed in their octahedral tilt structures. A suppression of the out-of-plane rotations of the TiO$_6$ octahedral in films grown on LSAT substrates resulted in a robust ferroelectric *I4 mm* phase with remnant polarization $\sim$5 μC/cm^2 at 10 K and T_c near 140 K. In contrast, films grown on NGO substrates with significant octahedral tilting showed reduced polarization and T_c. These results highlight the key role played by symmetry in controlling the ferroelectric properties of perovskite oxide thin films. © 2015 AIP Publishing LLC. [http://dx.doi.org/10.1063/1.4918805]

Calcium titanate (CaTiO$_3$) is the prototype for the perovskite structure. However, at room temperature, CaTiO$_3$ has the orthorhombic GdFeO$_3$ crystal structure ($a = 5.38$ Å, $b = 5.44$ Å, $c = 7.65$ Å) and only exhibits the cubic ($Pm\bar{3}m$) perovskite structure above $\sim$1575 K. Below this temperature, it takes the tetragonal *I4/mcm* structure and then transitions to the orthorhombic *Pnmb* structure below $\sim$1525 K.[1,2] It has been shown that the orthorhombic *Pnmb* tilt structure can be altered using epitaxial strain in thin films,[3,4] where the symmetry changes at the phase transitions are due to tilting of the TiO$_6$ oxygen octahedral away from cubic symmetry. The $Pm\bar{3}m$ to *I4/mcm* transition results from out-of-phase rotations of the octahedra around the c-axis, from $a^0a^0a^0$ to $a^0a^0c^-$ tilts according to Glazer notation.[5] The *I4/mcm* to *Pnmb* phase transition involves a change from out-of-phase to in-phase tilts along the c-axis and additional out-of-phase tilts along the a- and b-axes, which can be represented by the $a^-a^-c^+$ tilt pattern.

CaTiO$_3$ is similar to ferroelectric titanates such as BaTiO$_3$ and PbTiO$_3$ in bonding and composition; however, it does not undergo any ferroelectric transitions. Rather, CaTiO$_3$ is an incipient ferroelectric, akin to KTaO$_3$ and SrTiO$_3$, in which it has a polar soft mode but does not exhibit a ferroelectric phase transition due to quantum fluctuations.[6,7] This instability can be overcome and a robust ferroelectric state can be created in bulk materials with the substitution of Ca with larger ions.[8] For SrTiO$_3$ and KTaO$_3$, the ferroelectric state can also be stabilized through epitaxial strain.[9,10] The instability of the ferroelectric state in CaTiO$_3$ has been shown to be correlated to the competition between octahedral rotations and displacement of the Ca and Ti ions. It was predicted that suppression of these octahedral tilts would stabilize the *P4 mm* structure and thus allow for a large polarization.[11] Recent calculations have shown that an epitaxial strain of $\sim$1.5% (tensile) can enhance the ferroelectric instability and lead to a ferroelectric state.[12,13] Experimental evidence of ferroelectricity in CaTiO$_3$ has been limited to extrinsic switching due to oxygen vacancies.[14]

In order to better understand the effects of contrasting strain states and in-plane symmetries of CaTiO$_3$ on the stabilization of ferroelectric properties, we examine the structural and ferroelectric properties of CaTiO$_3$ thin films grown on orthorhombic (101)-oriented NdGaO$_3$ (NGO) and cubic (001)-oriented La$_{0.18}$Sr$_{0.82}$Al$_{0.65}$Ta$_{0.35}$O$_3$ (LSAT) substrates. These substrates have nearly identical pseudo-cubic lattice parameters, but differing octahedral tilt structures. The octahedral tilt structures imprinted into the CaTiO$_3$ films were determined by mapping intensities of half order Bragg peaks and scanning transmission electron microscopy (STEM). Both experiment and phase-field modeling indicate that the combined effects of the suppression of octahedral tilts and epitaxial strain lead to robust ferroelectric properties in thin films grown on LSAT substrates.

CaTiO$_3$ films were grown by pulsed laser deposition on LSAT and NGO substrates with lattice parameters a_{LSAT} = 3.87 Å, a_{NGO} = 5.43, b_{NGO} = 5.50 Å, and c_{NGO} = 7.71 Å. The films were grown in 100 mTorr pressure at 650 °C with

a)Present address: School of Materials, the University of Manchester, Manchester M13 9PL, United Kingdom.
b)ytakamura@ucdavis.edu

a laser fluence of 1.5 J/cm^2 from a CaTiO$_3$ ceramic target. These conditions were optimized to ensure the structural properties and cation stoichiometry of the films. The films have roughness of approximately 1 unit cell and grew in a layer-by-layer growth mode as evidenced from reflection high energy electron diffraction oscillations. The film thickness was limited to ∼10 nm to prevent relaxation of the epitaxial strain which was found to occur for thicknesses exceeding ∼20 nm. X-ray diffraction indicated that both films were fully commensurate with the substrate with cube-on-cube-type epitaxy. In Fig. 1(a), the out-of-plane lattice spacing for the films grown on LSAT substrates was found to be slightly smaller with a pseudo-cubic lattice parameter, $c_{PC} = 3.801 \pm 0.002$ Å, as compared to films on NGO substrates with $c_{PC} = 3.816 \pm 0.002$ Å, yet both films exhibit thickness fringes indicative of a smooth surface. From reciprocal space maps (not shown), the in-plane lattice constants for films on LSAT substrates were determined to be $a_{PC} = b_{PC} = 3.868 \pm 0.002$ Å, yielding an in-plane strain of 1.2%, while CaTiO$_3$ films grown on NGO substrates have $a_{PC} = 3.855 \pm 0.003$ Å and $b_{PC} = 3.865 \pm 0.003$ Å, giving an average in-plane strain of ∼1.1%. Though both films have similar strain states with nearly identical unit cell volumes, their crystal structures differ markedly, as seen by scans around the 202$_{PC}$-type peaks (Figs. 1(b) and 1(c)). CaTiO$_3$ films on LSAT substrates show nearly overlapping scans along the orthogonal 202$_{PC}$ and 022$_{PC}$ directions indicating a tetragonal-like structure. In contrast, similar scans for CaTiO$_3$ films grown on NGO substrates show three distinct lattice spacings along different 202$_{PC}$-type directions (orthorhombic 004, 242, and 400 reflections) indicating a monoclinic structure.

In order to accurately determine the intensities of the weak half integer peaks that correspond to the oxygen octahedral tilts, these films were examined using high brightness synchrotron based diffraction.[15,16] Since NGO and bulk CaTiO$_3$ share the same *Pnmb* space group, both substrate and thin film half order peaks are present as shown in Figures 2(a)–2(c). The observed peaks corresponded to reflections with *hkl* indices of the form (odd-even-odd)/2 and (odd-odd-odd)/2.[15] The $\frac{3}{2}\,2\,\frac{5}{2}$ peak (Fig. 2(a)) corresponds to in-phase tilts along the *b*-axis (i.e., b^+ tilts). In contrast, the $\frac{3}{2}\frac{3}{2}\frac{5}{2}$ and $\frac{1}{2}\frac{5}{2}\frac{5}{2}$ peaks correspond to tilts along the *a*- and *c*-axes, respectively, that are antiphase, i.e., neighboring octahedra along these axes tilt in opposite directions. The $\frac{1}{2}\frac{5}{2}\frac{5}{2}$ peak is much

weaker than the $\frac{3}{2}\frac{3}{2}\frac{5}{2}$ peak, indicating that the c^- tilts are greatly reduced. These results show that the film possesses the $a^-b^+c^-$ tilt structure with out-of-plane tilts greatly reduced from bulk symmetry. This finding is in agreement with the previous work asserting that the octahedral tilt structure for tensile-strained *Pnmb* SrRuO$_3$ films on NGO substrates yielded an $a^-b^+c^0$ or $a^-b^+c^-$ tilt structure.[4] Thus, the 1% tensile strain state suppresses the out-of-plane tilts but CaTiO$_3$ films grown on NGO substrates still remain members of the *Pnmb* space group.[15] In contrast, CaTiO$_3$ films grown on LSAT substrates possess a strikingly different octahedral tilt structure. Only half order peaks of the (odd-even-odd)/2 or (even-odd-odd)/2 type are present, indicating that the octahedral tilt structure has in-phase tilts around the in-plane directions and suppressed tilting around the out-of-plane direction. Moreover, these films appear to be twinned since all half order peaks are doublets as seen in Figures 2(d) and 2(e). This twinning is consistent with the fact that the LSAT substrate has equal in-plane lattice constants and therefore lends no preferred in-plane orientation allowing the CaTiO$_3$ film to twin around the *c*-axis. These twins are consistent with 110-type twin boundaries which are prevalent in bulk CaTiO$_3$.[17] The pairs of half order peaks have nearly equal intensities, indicating approximately equal proportions of both domains. This result strongly suggests that CaTiO$_3$ films on LSAT substrates assume the *P4$_2$/nmc* or *I4/mmm* space group, depending on whether the tilting is maintained along the *c*-axis.

The octahedral tilts in the CaTiO$_3$ films were further investigated by STEM high angle annular dark field (HAADF) and annular bright field imaging (ABF) along the pseudo-cubic [010]$_{pc}$ direction. HAADF and ABF STEM images were taken using an aberration-corrected Nion UltraSTEM operating at 200 kV, equipped with a cold field-emission electron gun and a corrector of third- and fifth-order aberrations. The convergence semi-angle for the electron probe was ∼30 mrad. ABF signals for the samples were collected from a detector angle range of ∼15–30 mrad, and the inner collection angle of HAADF images was 63 mrad. Figure 3 shows that although the interfaces of the CaTiO$_3$ films on both the LSAT and NGO substrates show a similar level of crystalline quality, the BO$_6$ octahedral connectivity at these two interfaces differs dramatically. The CaTiO$_3$/NGO interface (Figs. 3(c) and 3(d)) maintains a nearly constant tilt angle (β) across the interface due to the common
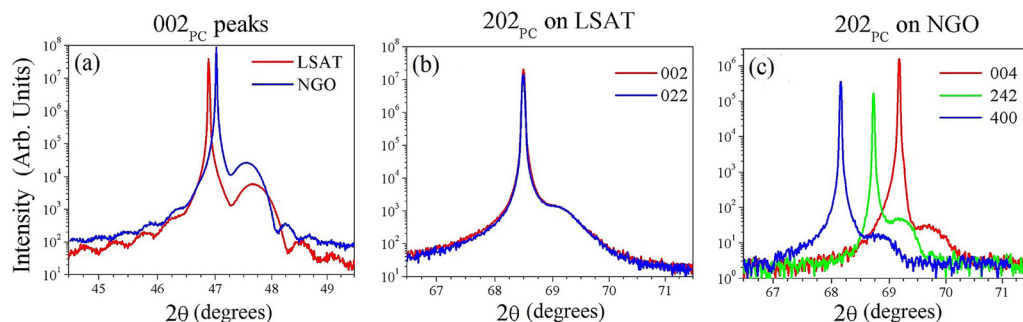

FIG. 1. (a) Out-of-plane diffraction around the 002$_{PC}$ peak showing the different lattice spacing for the films grown on LSAT and NGO substrates. The diffraction from orthogonal 202$_{PC}$ type peaks for the film grown on (b) LSAT and (c) NGO substrates indicating a tetragonal structure of CaTiO$_3$ grown on LSAT and a monoclinic structure for the films grown on NGO.
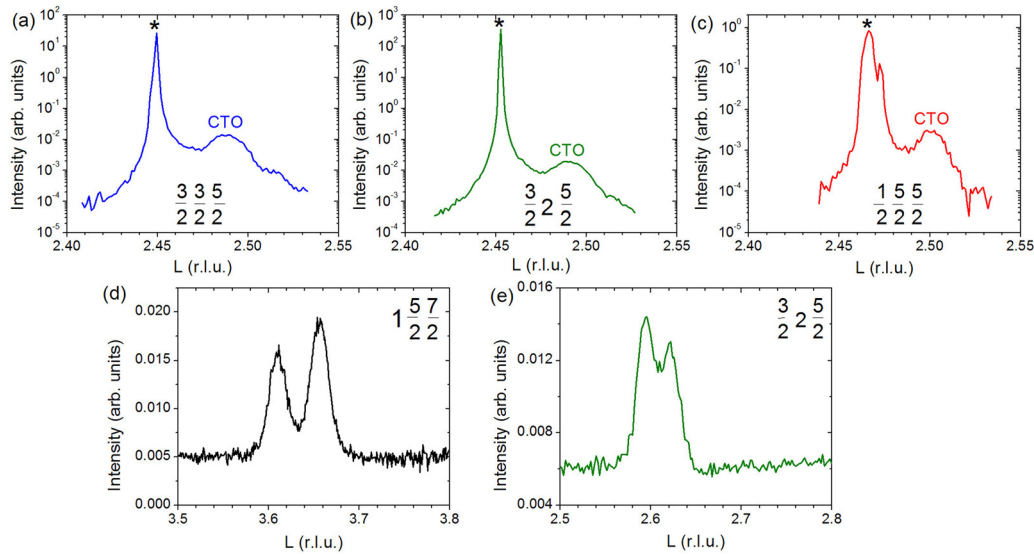
FIG. 2. *L*-scans around the (a) $\frac{3}{2}\frac{3}{2}\frac{5}{2}$, (b) $\frac{3}{2}2\frac{5}{2}$, and (c) $\frac{1}{2}\frac{5}{2}\frac{5}{2}$ half order peaks for CaTiO$_3$ films grown on NGO substrates. Substrate peaks are denoted by (*) and film peaks by (CTO). *L*-scans around the (d) $1\frac{5}{2}\frac{7}{2}$ and (e) $\frac{3}{2}2\frac{5}{2}$ half order peaks for CaTiO$_3$ films grown on LSAT substrates. The doublet features on the peaks suggest that the film has a twinned structure.

symmetry (*Pnmb* for both CaTiO$_3$ and NGO), consistent with synchrotron diffraction data. However, the CaTiO$_3$/LSAT interface (Figs. 3(a) and 3(b)) clearly exhibits a transition region across which β varies from zero in the cubic LSAT substrate (*Pm$\bar{3}$m*) to a bulk CaTiO$_3$ value (*Pnmb*) over a distance of ~7 atomic rows.

Given that the tilts in these materials are strongly coupled to the suppression of the ferroelectric transition, the differing octahedral tilt structures of CaTiO$_3$ films grown on LSAT and NGO substrates is expected to lead to disparate

FIG. 3. STEM-HAADF and ABF images of (a) CaTiO$_3$/LSAT and (c) CaTiO$_3$/NGO interfaces, viewed from the [010]$_{PC}$ zone axis. Polyhedral models showing the octahedral tilts are overlaid on the images. The size bar is 1 nm. BO$_6$ rotation angle, β for (b) CaTiO$_3$/LSAT and (d) CaTiO$_3$/NGO interfaces. The angles are projected onto the [010]$_{PC}$ direction and displayed as a plane averaged value. Adjacent BO$_6$ octahedra, which rotate in opposite directions, are denoted separately as red and black symbols. The dashed lines represent the CaTiO$_3$ bulk value along this axis.

ferroelectric properties. To compare the dielectric and ferroelectric properties of these films, they were measured with interdigitated electrodes to obtain the polarization in the plane of the film.[18] Despite theoretical predictions that a strain of at least 1.5% is needed to induce a ferroelectric state,[12,13] both of these films with lower strain exhibit ferroelectricity at low temperatures. Figure 4 shows peaks in the dielectric properties for films on both LSAT and NGO substrates; however, the temperatures of the maximum (T_{max}) differ. For films on LSAT substrates, T_{max} is ~140 K; for films grown on NGO, T_{max} is ~70 K. The ferroelectric behavior was also confirmed with polarization-electric field hysteresis loops at 10 K showing remnant polarizations of 5 and 1.5 μC/cm^2 for films on LSAT and NGO substrates, respectively. This difference in ferroelectric transition temperature and polarization is much larger than is expected for a ~0.1% change in strain state.[12,13] This discrepancy along with the measured differences in symmetry strongly suggest that, unlike what has been reported for theoretical calculations of epitaxial strain effects,[12,13] the suppression/alteration of the octahedral tilts plays a crucial role in inducing ferroelectricity in CaTiO$_3$. Underestimation of transition temperatures and overestimation of strains required to achieve the ferroelectric state in CaTiO$_3$ in the current theoretical framework can perhaps be attributed to the assumption that the room temperature paraelectric state is (001)-oriented orthorhombic *Pnmb* structure for the calculations,[12] whereas this work clearly shows a (101)-orientation for orthorhombic *Pnmb* CaTiO$_3$ on NGO substrates and a tetragonal symmetry for CaTiO$_3$ on LSAT substrates.

To further explore the effects of different symmetries on the predicted ferroelectric transition in CaTiO$_3$, a thermodynamic analysis was performed to calculate the strain dependent ferroelectric phase diagram with different symmetries in the paraelectric state. The previously determined thermodynamic potential from Gu *et al.*[13] was utilized to describe the coupling between the antiferrodistortive and ferroelectric phases in CaTiO$_3$. The phase transitions are described with a
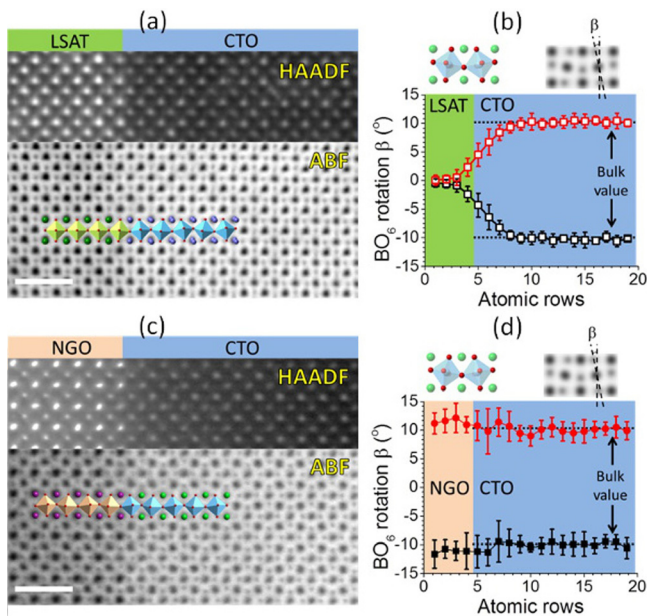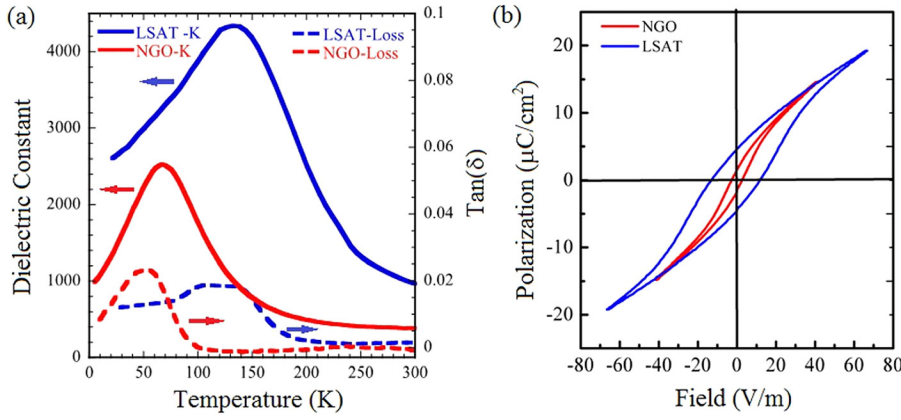
FIG. 4. (a) Dielectric properties vs. temperature for CaTiO$_3$ films measured at 1 kHz and (b) ferroelectric hysteresis loops at 10 K.

single Landau free energy expansion in terms of ε_i, P_i, θ_i, and φ_i, where ε_i ($i = 1$–6) are the strain components using Voigt's convention; P_i ($i = 1, 2, 3$) represent the three components of the spontaneous polarization in the Cartesian coordinate system; and θ_i and φ_i ($i = 1, 2, 3$) represent the in-phase and out-of-phase oxygen octahedral tilt components, respectively. The free energy can be described as follows:

$$
\begin{aligned}
F\big(P_i, \varphi_i, \theta_i, \varepsilon_{ij}\big) \\
= \alpha_{ij}P_iP_j + \alpha_{ijkl}P_iP_jP_kP_l + \alpha_{ijklmn}P_iP_jP_kP_lP_mP_n \\
- \mu_{ijkl}\varphi_i\varphi_j\theta_k\theta_l + \beta_{ij}\varphi_i\varphi_j + \beta_{ijkl}\varphi_i\varphi_j\varphi_k\varphi_l \\
+ \beta_{ijklmn}\varphi_i\varphi_j\varphi_k\varphi_l\varphi_m\varphi_n - \kappa_{ijkl}P_iP_j\theta_k\theta_l \\
+ \gamma_{ij}\theta_i\theta_j + \gamma_{ijkl}\theta_i\theta_j\theta_k\theta_l + \gamma_{ijklmn}\theta_i\theta_j\theta_k\theta_l\theta_m\theta_n - t_{ijkl}P_iP_j\varphi_k\varphi_l \\
+ \frac{1}{2}c_{ijkl}\varepsilon_{ij}\varepsilon_{kl} - g_{ijkl}\varepsilon_{ij}P_kP_l - \lambda_{ijkl}\varepsilon_{ij}\varphi_k\varphi_l - \varsigma_{ijkl}\varepsilon_{ij}\theta_k\theta_l,
\end{aligned} \tag{1}
$$

where α, β, and γ are Landau-Devonshire coefficients (only coefficients of the second order terms are temperature dependent) of polarization, out-of-phase tilt, and in-phase tilt, respectively; t_{ijkl}, κ_{ijkl}, g_{ijkl}, μ_{ijkl}, λ_{ijkl}, and ς_{ijkl} are coupling coefficients; c_{ijkl} is the elastic stiffness tensor. The indices i, j, k, and l run from 1 to 3. All the coefficients are defined as previously reported.[13] Since the films are (001)$_{PC}$-oriented, the coordinate system was rotated such that the x_1, x_2, and x_3 directions correspond to the $[\bar{1}10]$, $[001]$, and $[110]$ orthorhombic directions, respectively. By applying the thin film boundary condition, i.e., $\varepsilon'_{11} = \varepsilon'_{22} = \varepsilon_s$, $\varepsilon'_{21} = \varepsilon'_{12} = 0$, $\sigma'_{13} = \sigma'_{23} = \sigma'_{33} = \sigma'_{31} = \sigma'_{32} = 0$, and minimizing the total free

energy with respect to epitaxial strain, ε_s, a temperature-strain phase diagram can be determined. The prime sign indicates rotated tensors, and σ_{ij} stand for the stress tensor. The calculations were performed as described in Refs. 13 and 19. Phase diagrams for the space groups were calculated as a function of strain for the *Pnmb* space group (i.e., $a^-b^+c^-$ tilts) for CaTiO$_3$ films grown on NGO substrates and both the *P4$_2$/nmc* ($a^+a^+c^-$) or *I4/mmm* ($a^+a^+c^0$) space groups for CaTiO$_3$ films on LSAT substrates. The ferroelectric states in these materials could not be determined in a straightforward manner through simply minimizing the free energy due to the fact that several phases with and without polarization were close in energy. To overcome this complication, the most likely phases were determined from the symmetry consideration as shown by Stokes *et al.*[20] This procedure leads to the most likely ferroelectric phase for films on NGO substrates being *Pmc2$_1$*. For films on LSAT substrates, the most likely phases are more complex; *P4$_2$mc* and *Aba2* being likely for the *P4$_1$/nmc* space group and *I4 mm*, *Fmm2*, and *Cm* phases being likely for the *I4/mmm* space group. These results are summarized in Figure 5 where ferroelectric transitions were determined as a function of strain for the three initial starting space groups. Figures 5(a) and 5(b) show that the ferroelectric transition is better described using the *I4/mmm* phase because the calculations over-predict the amount of strain required to induce the phase transition for the *P4$_2$/nmc* phase. These results are consistent with the experimentally determined transition temperatures, though the results do not match precisely perhaps due to uncertainty in the coefficients used to describe CaTiO$_3$, as seen previously for the
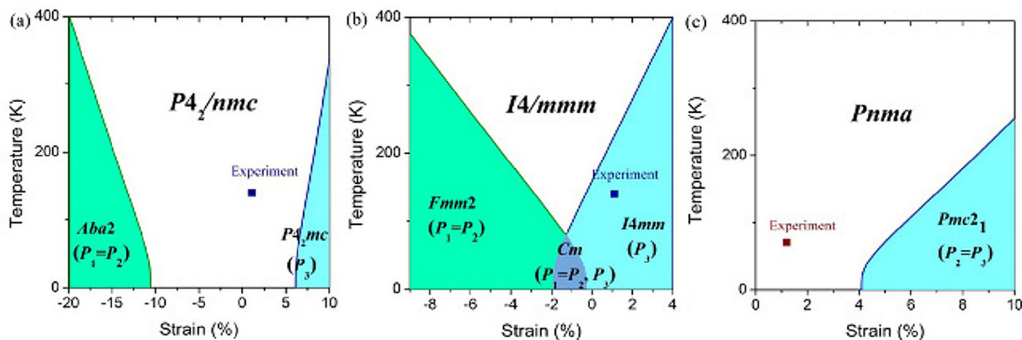

FIG. 5. The calculated temperature-strain phase diagram for CaTiO$_3$ films grown on (a) and (b) LSAT and (c) NGO substrates. The corresponding measured experimental transition temperatures are indicated on the phase diagrams.

calculation of transition temperatures in strained $SrTiO_3$.[9] Additional experiments would be required to better refine the values of these coefficients.

In conclusion, epitaxial $CaTiO_3$ thin films grown on LSAT and NGO substrates display strong ferroelectric properties in agreement with theoretical predictions. These substrates induce different symmetries and octahedral tilt structures in the films. The tensile strain imposed by both substrates strongly suppresses the octahedral tilts around the c-axis; however, distinct tilt ordering was observed with a twinned $a^+a^+c^0$ tilt structure for films grown on LSAT substrates and the $a^-b^+c^-$ tilt structure on NGO substrates. Ferroelectric and dielectric measurements show that the larger suppression of tilts on LSAT substrates results in a more robust ferroelectric state with remnant polarization $\sim$5 μC/cm^2 at 10 K and T_c near 140 K. However, unlike previous calculations, the in-plane symmetry of the epitaxial films affected the ferroelectric phase transition. This work demonstrates an innovative mechanism for controlling ferroelectricity by altering octahedral tilts in perovskites, not via direct interfacial coupling as recently investigated by several groups for regions just a few unit cells from the interface, but by macroscopic strain and control of strain symmetry. This tool has the potential to be applied to a wide range of orthorhombic *Pnmb* perovskite materials.

[1]B. J. Kennedy, C. J. Howard, and B. C. Chakoumakos, J. Phys.-Condens. Matter **11**, 1479 (1999).

[2]M. Yashima and R. Ali, Solid State Ionics **180**, 120–126 (2009).

[3]J. He, A. Borisevich, S. V. Kalinin, S. J. Pennycook, and S. T. Pantelides, Phys. Rev. Lett. **105**(22), 227203 (2010).

[4]A. Vailionis, H. Boschker, W. Siemons, E. P. Houwman, D. H. A. Blank, G. Rijnders, and G. Koster, Phys. Rev. B **83**(6), 064101 (2011).

[5]A. M. Glazer, Acta Crystallogr., Sect. B **28**, 3384 (1972).

[6]V. V. Lemanov, A. V. Sotnikov, E. P. Smirnova, M. Weihnacht, and R. Kunze, Solid State Commun. **110**, 611 (1999).

[7]T. Nakamura, P. H. Sun, Y. J. Shan, Y. Inaguma, M. Itoh, I. N. Kim, J. H. Sohn, M. Ikeda, T. Kitamura, and H. Konagay, Ferroelectrics **196**, 205 (1997).

[8]V. V. Lemanov, A. V. Sotnikov, E. P. Smirnova, and M. Weihnacht, Appl. Phys. Lett. **81**, 886 (2002).

[9]J. H. Haeni, P. Irvin, W. Chang, R. Uecker, P. Reiche, Y. L. Li, S. Choudhury, W. Tian, M. E. Hawley, B. Craigo, A. K. Tagantsev, X. Q. Pan, S. K. Streiffer, L. Q. Chen, S. W. Kirchoefer, J. Levy, and D. G. Schlom, Nature **430**, 758 (2004).

[10]M. Tyunina, J. Narkilahti, M. Plekh, R. Oja, R. M. Nieminen, A. Dejneka, and V. Trepakov, Phys. Rev. Lett. **104**, 227601 (2010).

[11]S. M. Nakhmanson, K. M. Rabe, and D. Vanderbilt, Phys. Rev. B **73**, 060101R (2006).

[12]C. J. Eklund, C. J. Fennie, and K. M. Rabe, Phys. Rev. B **79**, 220101 (2009).

[13]Y. Gu, K. M. Rabe, E. Bousquet, V. Gopalan, and L. Q. Chen, Phys. Rev. B **85**, 064117 (2012).

[14]S. M. Yang, S. J. Moon, T. H. Kim, and Y. S. Kim, Curr. Appl. Phys. **14**, 757–760 (2014).

[15]A. M. Glazer, Acta Crystallogr., Sect. A **31**, 756–762 (1975).

[16]S. J. May, J.-W. Kim, J. M. Rondinelli, E. Karapetrova, N. A. Spaldin, A. Bhattacharya, and P. J. Ryan, Phys. Rev. B **82**, 014110 (2010).

[17]H. F. Kay and P. C. Bailey, Acta Crystallogr. **10**, 219 (1957).

[18]M. D. Biegalski, Y. Jia, D. G. Schlom, S. Trolier-McKinstry, S. K. Streiffer, V. Sherman, R. Uecker, and P. Reiche, Appl. Phys. Lett. **88**, 192907 (2006).

[19]Y. L. Li, S. Choudhury, J. H. Haeni, M. D. Biegalski, A. Vasudeyarao, A. Sharan, H. Z. Ma, J. Levy, V. Gopalan, S. Trolier-McKinstry, D. G. Schlom, Q. X. Jia, and L. Q. Chen, Phys. Rev. B **73**, 184112 (2006).

[20]H. T. Stokes, E. H. Kisi, D. M. Hatch, and C. J. Howard, Acta Crystallogr., Sect. B **58**, 934 (2002).